Konno et al., http://www.jcb.org/cgi/content/full/jcb.201506123/DC1

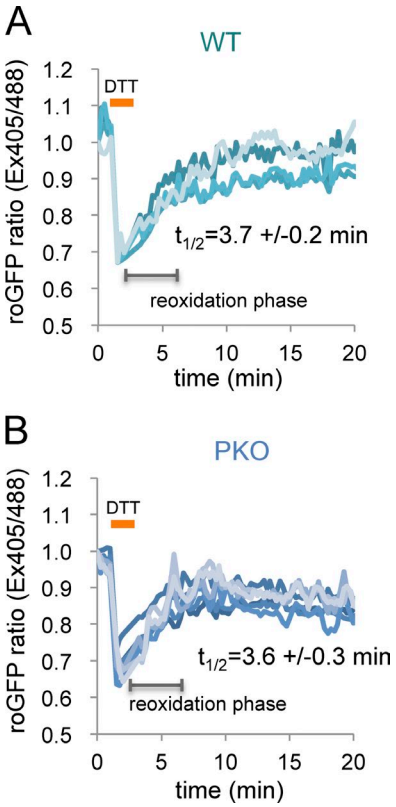

Figure S1. **No evidence for a contribution of PRDX4 to the rate of disulfide bond formation in ERO1-expressing cells.** (A and B) Traces of time-dependent changes in the fluorescence excitation ratio, reflecting the alterations in the oxidation state of roGFP2 expressed in the ER of PKO mouse lung fibroblasts or their isogenic control (WT). Cells were exposed to a brief (1 min) reductive pulse (DTT, 2 mM) followed by a washout. Each line traces the ratio in an individual cell (values shown denote mean recovery $t_{1/2}$ ± SEM, $n > 10$).

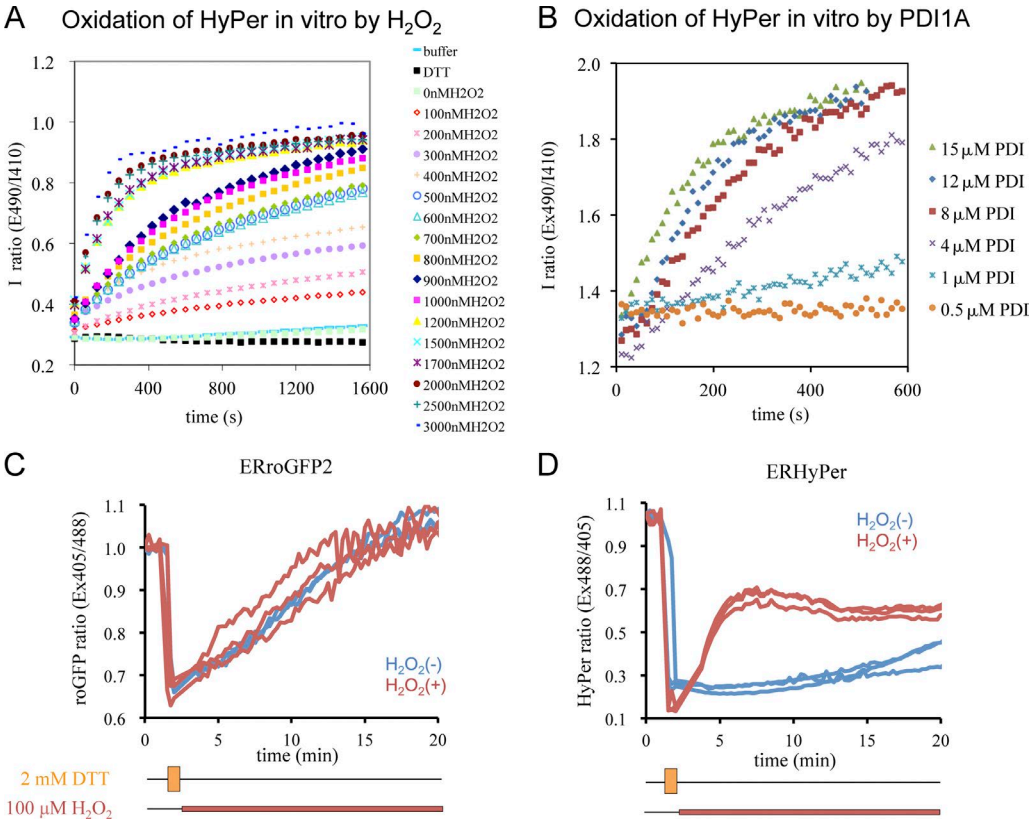

Figure S2. **Kinetics of HyPer oxidation by H_2O_2 or PDI in vitro and in vivo.** (A and B) Trace of time-dependent changes in the fluorescence excitation ratio of reduced HyPer (1 mM) exposed to the indicated concentrations of H_2O_2 (A) or oxidized PDI (B) in vitro and of roGFP2 (C) or HyPer (D) expressed in the ER of cells lacking ERO1 and PRDX4 (MEF^{TKO}); a brief (1 min) reductive pulse (DTT, 2 mM) was followed by a washout, during which H_2O_2 (100 mM) was added. Shown are traces of the ratio in individual cells. WT, wild type.

Table S1. **List of plasmids**

ID[a]	Plasmid name	Description	Reference	First appearance	Label in figure
1052	FLAGM1_roGFP2_pCDNA3.1	Mammalian expression, ER-localized roGFP2	Tsunoda et al., 2014	Fig. 1	ERroGFP2
1187	mPRDX4_37-274_WT_pFLAG_CMV1	Mammalian expression of mouse PRDX4	This study	Fig. 1	$PRDX4^{wt}$
1188	mPRDX4_37-274_C127S_pFLAG_CMV1	Mammalian expression of mouse PRDX4 inactive mutant	This study	Fig. 1	$PRDX4^{C127S}$
233	hPDI(18-508)pTrcHis-A	Bacterial expression of human PDI1A	Zito et al., 2010	Fig. 2	PDI
778	pHyper_pQE30	Bacterial expression HyPer	Belousov et al., 2006	Fig. 2	HyPer
855	pFLAG_ERHyPerA233V_CMV1	Mammalian expression, cytosolic HyPer2	This study, based on Markvicheva et al., 2011	Fig. 2	ERHyPer
1361	Cyto HyPer_A233V	Mammalian expression, mitochondrial HyPer2	This study, based on Markvicheva et al., 2011	Fig. 3	cytoHyPer
1362	Mito HyPer_A233V	Mammalian expression, ER targeted HyPer2	This study, based on Markvicheva et al., 2011	Fig. 3	mitoHyPer
1402	hCatase_cyto_pCEFL_mCherry	Mammalian expression of cytosolic human catalase and mCherry from separate promoters	This study	Fig. 4	cytoCat
1404	hCatase_mito_pCEFL_mCherry	Mammalian expression of mitochondrial human catalase and mCherry from separate promoters	This study	Fig. 4	mitoCat
1438	hCatase_ER_pCEFL_mCherry	Mammalian expression of ER human catalase and mCherry from separate promoters (ER active variant)	This study, based on Lortz et al., 2015	Fig. 4	ERCat

[a]Unique plasmid identification number used internally (a lab number).

References

Belousov, V.V., A.F. Fradkov, K.A. Lukyanov, D.B. Staroverov, K.S. Shakhbazov, A.V. Terskikh, and S. Lukyanov. 2006. Genetically encoded fluorescent indicator for intracellular hydrogen peroxide. *Nat. Methods.* 3:281–286. http://dx.doi.org/10.1038/nmeth866

Lortz, S., S. Lenzen, and I. Mehmeti. 2015. N-glycosylation-negative catalase: a useful tool for exploring the role of hydrogen peroxide in the endoplasmic reticulum. *Free Radic. Biol. Med.* 80:77–83. http://dx.doi.org/10.1021/bi800498g

Markvicheva, K.N., D.S. Bilan, N.M. Mishina, A.Y. Gorokhovatsky, L.M. Vinokurov, S. Lukyanov, and V.V. Belousov. 2011. A genetically encoded sensor for H2O2 with expanded dynamic range. *Bioorg. Med. Chem.* 19:1079–1084. http://dx.doi.org/10.1016/j.bmc.2010.07.014

Tsunoda, S., E. Avezov, A. Zyryanova, T. Konno, L. Mendes-Silva, E. Pinho Melo, H.P. Harding, and D. Ron. 2014. Intact protein folding in the glutathione-depleted endoplasmic reticulum implicates alternative protein thiol reductants. *eLife.* 3:e03421.

Zito, E., E.P. Melo, Y. Yang, Å. Wahlander, T.A. Neubert, and D. Ron. 2010. Oxidative protein folding by an endoplasmic reticulum-localized peroxiredoxin. *Mol. Cell.* 40:787–797. http://dx.doi.org/10.1016/j.molcel.2010.11.010